Journal of Neurochemistry

JOURNAL OF NEUROCHEMISTRY | 2014 | 131 | 484–497 doi: 10.1111/jnc.12839

ORIGINAL ARTICLE

Cannabinoid receptor 1 modulates the autophagic flux independent of mTOR- and BECLIN1-complex

Christof Hiebel, Tanja Kromm, Marcel Stark and Christian Behl

Institute for Pathobiochemistry, University Medical Center, Johannes Gutenberg University Mainz, Mainz, Germany

Abstract

Cannabinoid Receptor 1 (CB1) has been initially described as the receptor for Delta-9-Tetrahydrocannabinol in the central nervous system (CNS), mediating retrograde synaptic signaling of the endocannabinoid system. Beside its expression in various CNS regions, CB1 is ubiquituous in peripheral tissues, where it mediates, among other activities, the cell's energy homeostasis. We sought to examine the role of CB1 in the context of the evolutionarily conserved autophagic machinery, a main constituent of the regulation of the intracellular energy status. Manipulating CB1 by siRNA knockdown in mammalian cells caused an elevated autophagic flux, while the expression of autophagy-related genes remained unaltered. Pharmacological inhibition of CB1 activity using Rimonabant likewise caused an elevated autophagic flux, which was independent of the mammalian target of rapamycin complex 1, a major switch in the control of canonical autophagy. In addition, knocking down coiled-coil myosin-like BCL2-interacting protein 1, the key-protein of the second canonical autophagy control complex, was insufficient to reduce the elevated autophagic flux induced by Rimonabant. Interestingly, lysosomal activity is not altered, suggesting a specific effect of CB1 on the regulation of autophagic flux. We conclude that CB1 activity affects the autophagic flux independently of the two major canonic regulation complexes controlling autophagic vesicle formation.

Keywords: autophagy, CB1, GPCR, non-canonical, peripheral.

J. Neurochem. (2014) **131**, 484–497.

Cannabis sativa has been used as medical plant in Chinese and Indian medicine for at least 4000 years, but the chemical structure of the major psychoactive substance Delta-9-tetrahydrocannabinol was only described and synthesized in the 1960s (Mechoulam and Gaoni 1965). It took additional 20 years to identify Delta-9-tetrahydrocannabinol-receptors and to clarify the structure of these two G-protein-coupled receptors named cannabinoid receptor 1 (CB1; Devane *et al.* 1988; Matsuda *et al.* 1990) and cannabinoid receptor 2 (CB2; Munro *et al.* 1993). CB2 is mainly expressed in peripheral immune cells like B cells and natural killer cells (Galiegue *et al.* 1995) but is also found in distinct cell types of the central nervous system (CNS) like microglia and neuronal cells in the brainstem (Walter *et al.* 2003; Van Sickle *et al.* 2005). CB1 is primarily expressed in neuronal cells of the CNS, where it exerts its well described function as a receptor for endocannabinoids mediating retrograde synaptic signal transduction (Wilson and Nicoll 2001). CB1 is also expressed in a variety of peripheral organs and tissues,

Received December 1, 2013; revised manuscript received July 21, 2014; accepted July 22, 2014.

Address correspondence and reprint requests to Christian Behl, Institute for Pathobiochemistry, University Medical Center, Johannes Gutenberg University Mainz, Duesbergweg 6, 55099 Mainz, Germany. E-Mail: cbehl@uni-mainz.de

Abbreviations used: ACPA, arachidonoyl cyclopropamide; AKT, serine/threonine protein kinase Akt; AMPK, AMP-activated protein kinase; ATG, autophagy-related; BafA1, bafilomycin A1; BECLIN1, coiled-coil myosin-like BCL2-interacting protein 1; CB1, cannabinoid receptor 1; CB2, cannabinoid receptor 2; CMA, chaperone-mediated autophagy; DMSO, dimethyl sulfoxide; ER, endoplasmatic reticulum; GFP, green-flourescent protein; HEK, human embryonic kidney; LAMP1, lysosomal-associated membrane protein 1; LAMP2, lysosomal-associated membrane protein 2; LC3, light chain 3 protein; LIR, LC3-interacting region; MAPK/ERK, mitogen activated kinase/extracellular regulated MAP kinase; mTORC1, mammalian target of rapamycin complex 1; mTOR, mammalian target of rapamycin; NS, nonsense; PE, phosphatidylethanolamine; PI3, phosphatidylinositol 3-phosphate; PIK3C3, class III PI3-kinase; qPCR, quantitative RT-PCR; RT-PCR, reverse-transcription PCR; SD, standard deviation; siRNA, small interfering RNA; SQSTM1, sequestosome 1; SR, SR141716 (Rimonabant); THC, Delta-9-tetrahydrocannabinol; UPS, ubiquitin proteasome system; Win2, WIN55,212-2.

where it modulates cellular metabolic processes independently of its influence on the appetite control system in the CNS (Benard *et al.* 2012; O'Keefe *et al.* 2013).

The term autophagy summarizes a number of evolutionarily highly conserved metabolic mechanisms in eukaryotic cells, which ultimately all end up in the degradation of material in the lysosomes. Two autophagic pathways, microautophagy and chaperone-mediated autophagy, sequester their cargo directly into the lysosomes either by invagination of the lysosomal membrane or via lysosomal-associated membrane protein 2a, the receptor for chaperone-mediated autophagy localized in the lysosomal membrane. In contrast, macroautophagy (hereafter referred to as autophagy) relies on the formation of double membrane vesicles, called autophagosomes, to deliver cytoplasmic proteins and organelles to the lysosomal degradation machinery (Tanida 2011). The initiation and nucleation of autophagosome formation is controlled by two major inductive protein complexes, the mammalian target of rapamycin (mTOR) complex 1 (mTORC1) and the coiled-coil myosin-like BCL2-interacting protein 1 (BECLIN1)-complex (Mizushima *et al.* 2011). The activity of the mTOR-kinase suppresses autophagosome formation and thereby this complex acts as a negative regulator of autophagy. Rapamycin induces autophagic activity by inhibiting mTOR phosphorylation at serine 2448 and thus preventing its kinase activity (Chiang and Abraham 2005). The second important pathway for the initiation and maturation of autophagic vesicles is triggered by a multi-protein complex build around the hub-protein BECLIN1, signaling via the lipid phosphatidylinositol 3-phosphate, which is synthesized by a part of this complex, namely the class III phosphatidylinositol 3-phosphate-kinase (PIK3C3, Vsp34 in yeast; Fimia *et al.* 2007; Itakura *et al.* 2008; Zhong *et al.* 2009).

Besides these two induction complexes, a number of autophagy-related (ATG) proteins are hierarchically organized to generate functional autophagic vesicles (reviewed in Mizushima *et al.* 2011). One crucial step in the maturation of such autophagosomes is the conjugation of phosphatidylethanolamine to autophagic adaptors like the light chain 3 protein (LC3, ATG8 in yeast). Unconjugated LC3 (LC3-I) is distributed throughout the cell, whereas phosphatidylethanolamine-conjugated LC3 (LC3-II) is specifically localized at the inner and in part also at the outer autophagosomal membrane. Autophagy receptors like p62/ sequestosome 1 (SQSTM1) (hereafter referred to as SQSTM1) and other proteins bind to autophagic substrates and simultaneously via the LC3-interacting region to LC3 (Pankiv *et al.* 2007; Kirkin *et al.* 2009). Lately, evidence accumulates that formation of autophagosomes does not necessarily require involvement of either mTOR- and BECLIN1-complexes or the hierarchical intervention of all ATG proteins, but that cells can also induce autophagic vesicle formation in a non-canonical fashion, bypassing one or more elements of the canonical pathway (reviewed in Codogno *et al.* 2012). Modulators of these non-canonical pathways are of great interest.

Regulation of the autophagic flux under certain physiological or pathological conditions, e.g. an imbalance of nutrient supply, is of particular interest in neuronal cells. CB1 is known to influence the cellular metabolism directly. In this study we provide evidence that CB1 signaling influences autophagy, which might help the cell to adjust to different metabolic states. We show that CB1 activity indeed alters the autophagic flux and that this modulatory activity is exerted in a non-canonical and mTOR- and BECLIN1-independent manner.

Methods

Reagents

Unless stated otherwise, all reagents were from regular commercial sources as mentioned in the methods descriptions.

Cell culture

Human embryonic kidney cells 293A (HEK 293A) were purchased from Invitrogen, Karlsruhe, Germany; HEK::D2eGFP cells have been described previously (Gamerdinger *et al.* 2009). HEK cells were maintained in Dulbecco's modified eagle medium (DMEM, #41965, Invitrogen) supplemented with 1 mM sodium pyruvate (Invitrogen) and 10% (v/v) fetal calf serum (FCS; PAA, Cölbe, Germany) at 37°C in a 5% CO_2-humidified atmosphere. Medium was refreshed every 3 days and 24 h prior to experiments.

Primary astrocytes of embryonal day 14 C57/Blc6n mouse embryos were prepared as described previously (Zschocke *et al.* 2005). Astrocyte cultures were maintained in minimal essential medium (#31095; Invitrogen) supplemented with 50 μg/mL gentamycin (#15750; Invitrogen) and 10% (v/v) heat-inactivated horse serum (Invitrogen) at 37°C in a 5% CO_2-humidified atmosphere. Astrocytes were split 48 h prior to experiments.

Plasmids, siRNA and transfection methods

Expression plasmid for green-flourescent protein (GFP)-LC3 was provided by Addgene (Jackson *et al.* 2005); expression plasmids for human CB1 (hCB1) and human CB2 (hCB2) were purchased from the Missouri S&T cDNA Resource Center; expression plasmid for eGFP-tagged hSOD1 (G85R) has been described previously (Witan *et al.* 2008). siRNAs were purchased from Eurofins-MWG-Operon (Ebersberg, Germany) as duplexes carrying 3′-dTdT overhangs. Specificity of knockdown effects were verified using two independent siRNA duplexes for each target gene and the same amount of a nonsense sequence as control (siRNA sequences are listed in Table S2).

Cells used for biochemical assays were transfected by electroporation in the Amaxa Nucleofector I (program T-24 for HEK cells, T-20 for astrocytes) using standard electroporation cuvettes (Sigma-Aldrich, Taufkirchen, Germany). A total of 30 μg of siRNA or plasmid was used for transfection, respectively. Cells were transfected in transfection buffer containing 135 mM KCl, 2 mM $MgCl_2$, 0.2 mM $CaCl_2$, 5 mM EGTA, 10 mM HEPES (pH 7.3), and 25% heat-inactivated FCS (PAA). CB1 siRNA knockdown was controlled by quantitative real-time reverse transcription PCR for every experiment (for the exact procedure, see other paragraph).

HEK cells used for immunocytochemistry were transfected using FuGene transfection reagent (Promega, Mannheim, Germany). Plasmids and siRNA were diluted in 1 mL of DMEM supplemented with 1 mM sodium pyruvate at RT. FuGene was pre-warmed to RT and filled up to a total volume of 1 mL using DMEM supplemented with 1 mM sodium pyruvate. FuGene and nucleic acid solutions were mixed dropwise, inverted several times and incubated for 15 min at RT. A total of 75 μL of transfection solution was used per well in a 24-well plate and 1 mL for a 60 cm^2 dish used for siRNA knockdown control. Cells were incubated for 72 h with transfection solution and washed once with pre-warmed culture medium. Bafilomycin A1 (BafA1; ENZO, Lörrach, Germany) treatment was performed using 1 μM BafA1 or dimethyl sulfoxide (DMSO) (Roth, Karlsruhe, Germany) as vehicle control diluted in fresh culture medium for 4 h at 37°C in a 5% CO_2-humidified atmosphere. Cells used for the aggregation assay were transfected utilizing calcium phosphate precipitation method (Graham and van der Eb 1973) using 10 μg of hSOD1(G85R)-expression plasmid and 30 μg of the indicated siRNA for each transient transfection.

Pharmacological treatments

Cells had been cultured under standard conditions for 24 h before medium was changed to DMEM supplemented with 1 mM sodium pyruvate and 10% (v/v) delipidized FCS (Lonza, Basel, Switzerland) 24 h prior to treatment. Treatment of cells with 100 nM Win55212-2 (Win2; Sigma-Aldrich) or 100 nM SR141716 [SR141716 (Rimonabant); a kind gift of Beat Lutz, Mainz] was performed in DMEM supplemented with 1 mM sodium pyruvate for 4 h. BafA1 (ENZO) treatment was performed subsequently using 1 μM BafA1 or DMSO (Roth) as vehicle control for 4 h at 37°C in a 5% CO_2-humidified atmosphere.

Reverse transcription PCR (RT-PCR), quantitative real-time RT-PCR (qPCR), and qPCR array analysis

RNA extraction, RT-PCR, and qPCR were performed as described previously (Stumm *et al.* 2013). Total RNA of cells was extracted using the Nucleospin RNA II Kit (Macherey-Nagel, Düren, Germany) according to the manufacturer's protocol. For reverse transcription (RT), 1 μg RNA of each preparation was diluted in 10 μL RNase-free water (Qiagen, Hilden, Germany), incubated at 65°C for 5 min using the iCycle thermocycler (Bio-Rad Laboratories, Munich, Germany) and then placed immediately on ice. RT-reaction was performed for 60 min at 37°C using the iCycle thermocycler (Bio-Rad) adding 10 μL of 2x RT mix (2 μL 10x RT-buffer [Qiagen], 2 μL dNTP mix [dATP, dCTP, dGTP, dTTP 5 mM each; Qiagen], 2 μL oligo-dT[15]-primer [10 μM; Promega], 1 μL RNasein [Promega], 1 μL reverse transcriptase [Qiagen], 2 μL RNase-free water [Qiagen]). RT-reactions for mock-controls were performed as described above substituting the reverse transcriptase with RNase-free water.

PCR was performed in a 25 μL reaction volume containing 2 μL cDNA, 0.1 μL forward and reverse primers (10 pmol each), 2.5 μL 10x PCR-buffer (Invitrogen), 0.75 μL $MgCl_2$ (50 mM; Invitrogen), 0.5 μL dNTP Mix (10 mM each; Peqlab, Erlangen, Germany), 0.2 μL *T.aq* polymerase (Invitrogen) and 19 μL water using the iCycle thermocycler (Bio-Rad). After 5 min of initial denaturation at 95°C, PCR conditions were 95°C for 30 s, 58°C for 30 s and 72°C for 30 s for 35 cycles. Primer sequences used for RT-PCR analysis are listed in Table S2. PCR products were analyzed by agarose gelelectrophoresis.

For relative quantification of mRNA, real-time PCR (qPCR) was performed in a 25 μL reaction volume containing 1 μL cDNA, 0.5 μL forward and reverse primers (10 pmol each), 12.5 μL of 2x Absolute qPCR SYBR Green Mix (Bioline, Luckenwalde, Germany) and 10.5 μL water using the iCycler real-time thermocycler (Bio-Rad). After 15 min of initial denaturation at 95°C, PCR conditions were 95°C for 30 s, 60°C for 30 s and 72°C for 30 s for 35 cycles. Ribosomal protein L19 (*rpl-19*) gene was used as reference gene for all experiments. Primer sequences used for qPCR analysis are listed in Table S2. The expression of 88 ATG genes was measured in two independent experiments using the human autophagy primer library-1 (Biomol, Hamburg, Germany) according to the manufacturer's protocol. Reaction volume [19 μL containing 1 μL cDNA, 10 μL of 2x Absolute qPCR SYBR Green Mix (Bioline) and 8 μL water] was added to 1 μL of the different human autophagy primer library-1 primer pairs per well in a 96 well plate. qPCR was performed using the iCycler real-time thermocycler (Bio-Rad). After 15 min of initial denaturation at 95°C, PCR conditions were 95°C for 30 s, 58°C for 30 s, and 72°C for 45 s for 35 cycles. The first PCR cycle that generated a flourescence signal above the threshold (Ct) was determined. The confirmation of PCR product specificity was done by analysis of the melting curves of each PCR product. Relative gene-expression was calculated using the relative expression software tool (Pfaffl *et al.* 2002).

Protein extraction and immunoblotting

Cells were washed with ice-cold phosphate-buffered saline (PBS, Invitrogen) and collected in ice-cold probe buffer [50 mM Tris-HCl, 10% sucrose, 1 mM EDTA, 1 mM EGTA, 15 mM HEPES pH 6.8, 1 mM sodium ortho-vanadate, 1 mM NaF, phosphatase-inhibitor cocktail (Roche, Basel, Switzerland), EDTA-free proteinase-inhibitor cocktail (Roche)]. Resuspended cells were subjected to sonication on ice 3 × 10 s using a tip-sonicator (Hielscher, Teltow, Germany), referred to as total lysate. Protein concentration was determined using the bicinchoninic acid assay (Thermo Scientific, Waltham, MA, USA) according to the manufacturer's protocol. Equal amounts of protein (15–30 μg) were adjusted and 5-fold loading buffer (10% sodium dodecyl sulfate, 20% glycerol, 125 mM Tris, 1 mM EDTA, 0.002% bromphenol-blue, 10% β-mercaptoethanol) was added. Samples were boiled for 5 min on 99°C and subsequently subjected to sodium dodecyl sulfate–polyacrylamide gel electrophoresis using hand-cast Bis-Tris gels with MES running buffer (Invitrogen) and transferred to nitrocellulose membranes. Membranes were incubated with Tris-buffered saline (TBS) containing 0.05% Tween20 (TBSt) and 4% non-fat dried milk powder (Applichem, Chicago, IL, USA) for 1 h at RT to block unspecific binding sites. All antibodies were dissolved in TBSt for incubation (primary antibodies are listed in Table S1). Proteins were detected by chemiluminescence using peroxidase-conjugated secondary antibodies (Jackson, listed in Table S1) and enhanced chemiluminescence-developing buffer [0.025% luminol (Sigma-Aldrich), 0.1 M Tris-HCl pH 8.6, 0.011% p-coumaric acid (Sigma-Aldrich), 0.3% H_2O_2]. Chemiluminescent signals were detected with the Fusion Imaging system (Peqlab) and quantified using ImageJ software (NIH, Bethesda, MD, USA).

Immunocytochemistry

Glass cover slips were incubated with 10 μg/mL poly-L-ornithine (Sigma-Aldrich) in 24-wells plates for 1 h at 37°C and subsequently washed twice with PBS (Invitrogen) and once with medium used for maintenance. HEK cells were grown on incubated glass cover slips, primary astrocytes were grown on plastic dishes (TPP, Trasadingen, Switzerland). Cells were fixed with ice-cold 4% para-formaldehyde (Sigma-Aldrich) in PBS for 15 min at RT. Permeabilization of HEK cells and blocking of unspecific binding sites was performed with TBS containing 0.1% Triton-X100 (Sigma-Aldrich) and 3% bovine serum albumin (BSA; Sigma-Aldrich) for 5 min at 4°C. Primary astrocytes were permeabilized using methanol on −20°C for 5 min, washed three times with TBS and blocked with TBS containing 3% BSA for 5 min at 4°C. Cells were incubated with primary antibodies (listed in Table S1) diluted in TBS containing 1% BSA at 4°C over night. Thereafter, cells were incubated with fluorophore-conjugated secondary antibodies (listed in Table S1) diluted in TBS containing 1% BSA for 1 h at RT. Microscopic analysis was performed with an inverted Axiovert 200 microscope (Zeiss, Munich, Germany) equipped with a SPOT RT CCD-camera (Diagnostic Instruments, Visitron, Puchheim, Germany). Laser scanning confocal microscopy was performed using the laser scanning confocal microscopy 710 ZEN system (Zeiss). LC3-puncta were counted in primary astrocytes either transfected with nonsense RNA or murine CB1 (mCB1) siRNA (as described above) and treated with 1 μM of BafA1 for 4 h prior to fixation. At least three different positions of the corresponding stainings per experiment were documented as maximum intensity projections of confocal laser scanning microscopy and counted numbers of LC3-puncta were averaged. Three independent experiments were performed. Cells for the protein aggregation assay were plated on culture dishes 24 h prior to transfection. Medium was exchanged to phenolred-free DMEM (#21063; Invitrogen) supplemented with 1 mM sodium pyruvate (Invitrogen) and 10% (v/v) FCS (PAA) 24 h after transfection. Cells, transfected cells and aggregates of five different positions of the corresponding treatment per experiment were documented 72 h after transfection. Counted numbers of aggregates and cells were averaged for each experiment. Four independent experiments were performed. For cell death/survival analysis, long-term starvation (15 h) was performed by incubating the cells either in aminoacid-free medium (phenolred-free Hank's Balanced Salt Solution #14025, Invitrogen; supplemented with 1 mM sodium pyruvate, Invitrogen) or phenolred-free DMEM (see above), 56 h after siRNA transfection. Dead cells were visualized utilizing propidium iodide (PI) incubation (1 μg/mL, 10 min) and documented subsequently. Five positions of each treatment were documented and total cell numbers as well as of PI-positive cells were counted and averaged. The percentage of dead cells was calculated from the number of PI-positive cells per total cell numbers in the optical field. Four independent experiments were performed.

Measurement of cathepsin activity

After transfection, 4000 cells per well were grown on poly-L-ornithine coated 96-wells plates 72 h prior to experiments. Medium was changed to phenolred-free DMEM (#21063; Invitrogen) supplemented with 1 mM sodium pyruvate (Invitrogen) and 10% (v/v) FCS (PAA) 24 h prior to experiments. Cells were incubated with 2 μM BafA1 (ENZO) or DMSO (Roth) as vehicle control for 4 h in 50 μL fresh phenolred-free DMEM per well. Subsequently, 50 μL phenolred-free DMEM containing 200 μM cathepsin substrate (Z-RR-AMC #BML-P137; ENZO) per well was added and cells were incubated for additional 1 h. After incubation with Z-RR-AMC medium was removed completely and cells were lysed in reporter lysis buffer (Promega) at −80°C for 1 h. After lysis the cell lysate was thawed for 30 min at 37°C and AMC fluorescence was recorded at 37°C in 3-min intervals for a total time period of 15 min using the Fluoroscan Ascent FL (Thermo Scientific).

Statistical analysis

Data are presented as mean ± SD. Data were analyzed by Student's *t*-test using SPSS software (IBM, New York, NY, USA). Differences were considered statistically significant if $*p < 0.05$, $**p < 0.01$ or $***p < 0.001$.

Results

Knockdown of CB1 via siRNA stimulates autophagic vesicle formation

Human embryonic kidney cells (HEK) express CB1 endogenously (Fig. 1a). A reduction by more than 50% of CB1 mRNA via siRNA transfection (si hCB1, Fig. 1c) led to an elevated autophagic flux (Fig. 1b and e). The autophagic flux was monitored by western blot analysis of the autophagic markers SQSTM1 and LC3-II. Treatment of HEK cells with BafA1 blocked lysosomal degradation efficiently and thereby led to an accumulation of autophagic vesicles (Fig. 2a) accompanied by an increase in LC3-II and SQSTM1 [compared to vehicle (DMSO) control], allowing to monitor the level of autophagy (Fig. 1b). BafA1 treatment resulted in a twofold increase of LC3-II in si hCB1 cells compared to nonsense siRNA [si nonsense (NS)] control cells (Fig. 1d) accompanied by an increase in the conversion of LC3-I into LC3-II (Figure S1a). Using pepstatin A and E64d (PepA/E64d) to block lysosomal degradation is similar to BafA1 treatment (Figure S1b and c). The autophagic flux is still elevated in CB1 knockdown condition if cells are subjected to amino acid starvation to induce autophagy (Figure S2a and b). Interestingly, cell death in CB1 knockdown cells is reduced after long-term starvation (15 h), measured by subsequent PI staining of the cells (Figure S2c and d). The elevated autophagic flux mediated by CB1 knockdown was not due to a transcriptional regulation of ATG genes including *lc3* or *p62/sqstm1* (Table S3). On the other hand, the activity of the ubiquitin proteasome system (UPS) as the second major principal protein degradation pathway (Clague and Urbe 2010) was not altered in HEK cells subjected to CB1 siRNA transfection. Proteasomal activity was monitored by using a stable-transgenic HEK cell line (HEK::D2eGFP) expressing D2eGFP, a reporter for UPS activity in living cells with a half-life of approximately 2 h. In a cyclohexamide chase experiment, the proteasomal degradation of D2eGFP in si hCB1 cells was unchanged compared to si NS cells (Figure S1d and e).

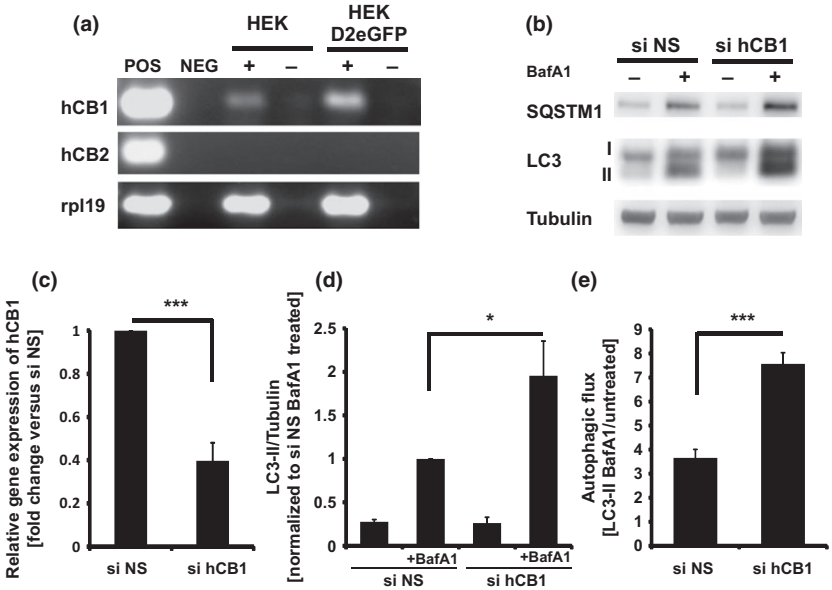

Fig. 1 Down-regulation of cannabinoid Receptor 1 (CB1) expression enhances the autophagic flux. (a) RT-PCR analysis revealed that human embryonic kidney (HEK) and HEK::D2eGFP cells (stable-transgenic HEK cells expressing proteasome reporter D2eGFP) endogenously express CB1 but no CB2 receptor mRNA. As positive controls (POS), 2 ng hCB1 in pcDNA3 vector, 2 ng hCB2 in pcDNA3 vector, or a RT-PCR amplificate of rpl19 from HEK cell RNA were used. The negative control (NEG) was the respective master mix without a template. + indicates RT-PCR of HEK or HEK::D2eGFP cells. – indicates the MOCK controls of the RT-PCR in which reverse transcriptase was substituted by RNAse free water. (b) Knockdown of CB1 expression led to an increased accumulation of light chain 3 protein (LC3)-II and sequestosome 1 (SQSTM1) in bafilomycin A1 (BafA1) treated (1 μM, 4 h) cells. (c) Residual level of CB1 mRNA after CB1 siRNA treatment was 40% of control [si nonsense (NS), nonsense siRNA] in average ($n = 8$). (d) Densitometric analysis revealed a significant increase in LC3-II in CB1 siRNA-treated cells compared to nonsense siRNA control. (e) The autophagic flux as measured by calculating the quotient of LC3-II level in BafA1 treated versus untreated cells was significantly enhanced in CB1 knockdown cells. Shown are means ± SD ($n = 3$). *$p < 0.05$; ***$p < 0.001$.

Next, we asked whether the elevated flux in CB1 knockdown cells had an influence on the degradation of known autophagic substrates. To address this point, we over-expressed mutant eGFP-tagged superoxide dismutase 1 G85R [SOD1(G85R)-eGFP], which initiates the formation of protein-aggregates that are degraded by the autophagosomal system (Gamerdinger *et al.* 2011b). Numbers of transfected cells analyzed per experiment and the total number of transfected cells counted over all experiments were similar between the two groups (Figure S1f). Less SOD1(G85R)-eGFP containing protein-aggregates occurred in cell cultures cotransfected with hCB1 siRNA (Fig. 2b and c) indicating an enhanced degradation of these autophagosomal substrates after induction of the autophagic flux via CB1 kockdown.

Pharmacological modulation of CB1 activity alters the autophagic flux

Next, we tested in pharmacological inhibition and stimulation experiments if it was the reduced level of CB1 protein or the reduced CB1 activity that caused the elevated autophagic flux observed after CB1 siRNA transfection. HEK cells incubated with 100 nM of the CB1-specific antagonist SR141716 (SR, Rimonabant) showed an elevated autophagic flux (Fig. 3) similar to the one found after si RNA knockdown of CB1 (Fig. 1). Treatment with 100 nM CB1/CB2 agonist WIN55,212-2 (Win2) had an opposite effect, as Win2 reduced the autophagic flux to 80% of vehicle (DMSO) control (Fig. 3a and c). HEK cells do not express CB2 (Fig. 1a) and therefore activation of CB1 is very likely causative for the effect of Win2 on the autophagic flux. The accumulation of LC3-II was more pronounced in SR-incubated cells and reduced in Win2-treated cells after subsequent BafA1 incubation compared to vehicle controls (Fig. 3b).

Reduced CB1 activity results in elevated autophagic vesicle formation in primary astrocytes

Next, we investigated the impact of a reduction in CB1 activity on the autophagic flux in primary astrocytes as these cells are non-transformed and do express CB1 endogenously. Inhibiting the receptors activity either by siRNA (Fig. 4a and b and Figure S3a) or pharmacologically by Rimonabant treatment (Fig. 4c and d) induced autophagic vesicle formation in the astrocyte cultures. The accelerated formation of autophagosomes because of CB1 siRNA knockdown is

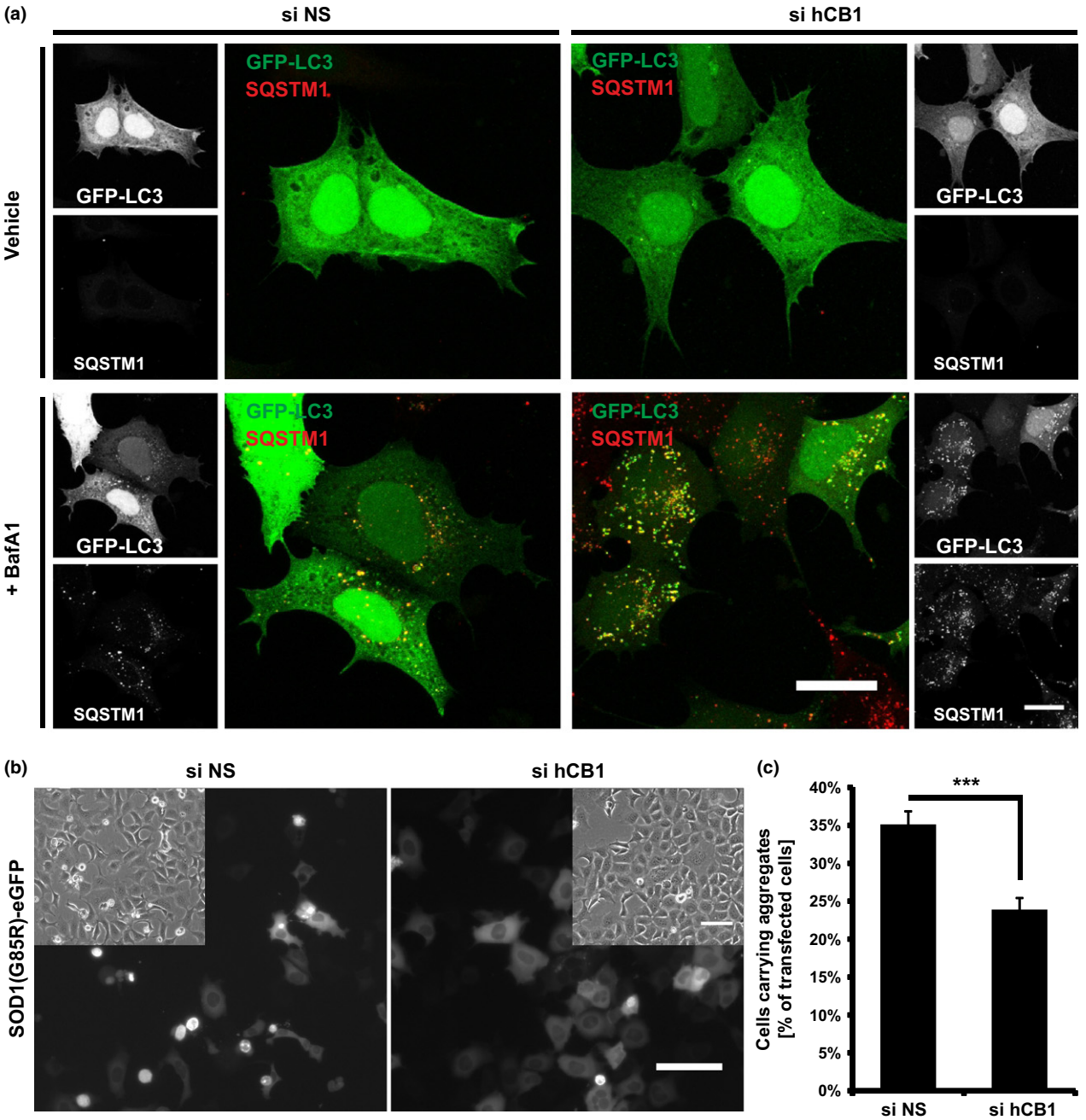

Fig. 2 (a) Knockdown of cannabinoid Receptor 1 (CB1) leads to increased autophagic vesicle formation. Shown are maximum intensity projections of confocal laser scanning microscopy of nonsense siRNA [si nonsense (NS)] or CB1 siRNA (si hCB1)-transfected cells. human embryonic kidney (HEK) cells were cotransfected with a green-flourescent protein (GFP)-light chain 3 protein (LC3) expression plasmid to mark successfully transfected cells and LC3 distribution within the cells (green). Sequestosome 1 (SQSTM1) was visualized by immunostaining (red). Scale bars = 20 μm. (b) Cells were cotransfected with SOD1(G85R)-eGFP expression plasmid and nonsense (si NS) or hCB1 siRNA (si hCB1), respectively. Scale bars = 100 μm (c) Number of cells carrying aggregates per total transfected cells is reduced after CB1 knockdown. Shown are the means ± SD ($n = 4$). ***$p < 0.001$.

also indicated by an increased number of LC3-positive puncta in CB1 knockdown cells compared to the control after BafA1 treatment (Fig. 4e and Figure S3b). This argues against a HEK- or clonal cell-specific effect of CB1 activity on the autophagic flux and is in line with the report of Piyanova *et al.* (2013), who observed an elevated autophagic vesicle formation in primary neuronal cultures of CB1-KO mice.

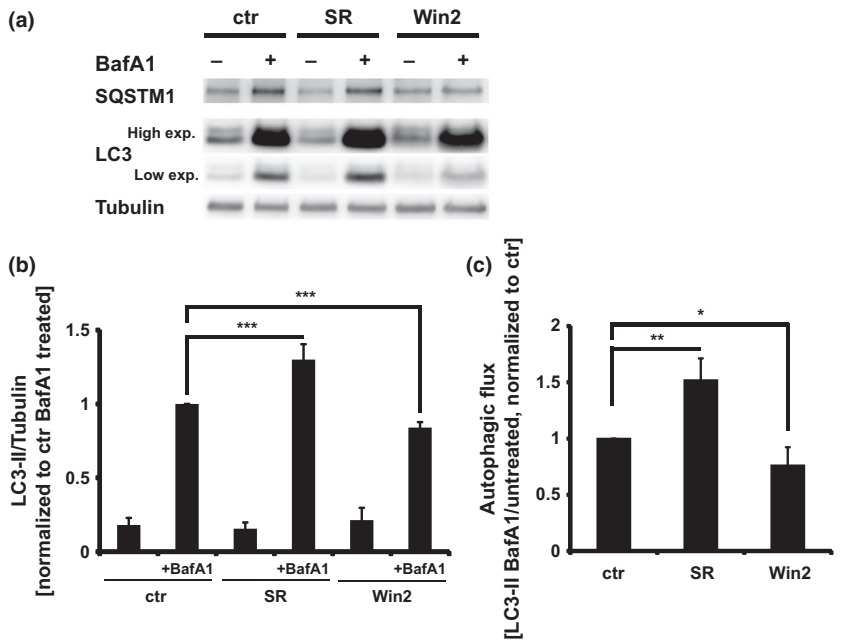

Fig. 3 Pharmacological modulation of cannabinoid Receptor 1 (CB1) activity alters the autophagic flux. (a) Human embryonic kidney (HEK) cells were treated with CB1 receptor antagonist SR141716 (SR, Rimonabant; 100 nM, 4 h) or agonist WIN 55,212-2 (Win2; 100 nM, 4 h) and lysosomal degradation was blocked subsequently by bafilomycin A1 (BafA1) treatment (1 μM, 4 h). (b) SR administration led to an increased accumulation of light chain 3 protein (LC3)-II and Win2 administration reduced the accumulation of LC3-II compared to vehicle control (ctr) in BafA1-treated cells. (c) The autophagic flux was enhanced in SR-treated cells and reduced in Win2-treated cells. Shown are the means ± SD ($n = 4$). $^{*}p < 0.05$; $^{**}p < 0.01$; $^{***}p < 0.001$.

CB1 modulates the autophagic flux independent of mTOR- and BECLIN1-complexes

The mTOR is one of the two major upstream protein complexes controlling autophagic activity. mTOR is a negative regulator of autophagy and therefore its activation leads to a suppression of autophagic vesicle formation. mTOR-phosphorylation at serine 2448 (S2448), which is inhibited by rapamycin, is widely used as a marker for mTOR activity (Chiang and Abraham 2005; Klionsky *et al.* 2012). Rapamycin prevented mTOR-phosphorylation at S2448 in HEK cells, confirming the sensitivity of the cells used for this study (Fig. 5a). The activity of the serine/threonine protein kinase Akt (AKT) is known to be regulated by CB1 (Cannich *et al.* 2004; Ozaita *et al.* 2007) and is stimulating mTOR activity (Dibble and Manning 2013). Thus, CB1 might exert its modulatory effect on the autophagic flux via the control of AKT. However, the transient knockdown of CB1 had no effect on AKT-phosphorylation on Serine 473 (p-AKT; Fig. 5f and g), which was used as a marker for AKT activity. Western blot analysis of the downstream mTOR total protein and phosphorylated mTOR (p-mTOR) served to clarify if CB1 knockdown modulated autophagic flux by altering mTOR activity independently of AKT. We found no difference in the total amount of mTOR protein between CB1 siRNA and nonsense siRNA transfected cells (Fig. 5a and b). The p-mTOR level was also not changed in si hCB1 cells compared to si NS control cells (Fig. 5a and c). BafA1 treatment (1 μM, 4 h) did not significantly alter mTOR total protein level or p-mTOR (Fig. 5a–c). In addition, the substrate of the mTOR kinase, the p70S6 kinase (S6K) (Dufner and Thomas 1999) showed no difference in its phosphorylation status on its mTOR-dependent phosphorylation-site at T389 upon CB1 knockdown (p-S6K, Fig. 5d and e). Next, we analyzed the activity of the ULK1 kinase, another substrate of the mTOR-kinase. ULK1 activity drives autophagy and is suppressed by mTOR because of phosphorylation at Serine 757 [p-ULK1 (S757), Mizushima 2010]. We found no difference in p-ULK1 (S757) between CB1 siRNA and nonsense siRNA transfected cells (Fig. 5h and i). As ULK1 might be regulated via direct phosphorylation by the AMP-activated protein kinase (AMPK) (Egan *et al.* 2011) we analyzed the AMPK-dependent phosphorylation-site of ULK1 at S555 [p-ULK1 (S555)] and observed no difference in p-ULK1 (S555) between CB1 knockdown and control cells (Fig. 5h and i).

The second major protein complex controlling autophagic activity is the BECLIN1-complex. Knockdown of BECLIN1 (si BECLIN1, Fig. 6a) protein or of the relevant kinase PIK3C3 (si PIK3C3, Fig. 6c and e) of this complex indeed reduced the autophagic flux (Fig. 6b and d) compared to nonsense siRNA (si NS) transfected cells. Again, incubation with CB1 antagonist Rimonabant (SR141716, 4 h 100 nM prior to BafA1 treatment) increased formation of autophagic vesicles (Fig. 6a and c) in si NS cells, but also in si BECLIN1 and si PIK3C3 transfected cells. Moreover, SR141716 treatment restored the autophagic flux in si BECLIN1 or si PIK3C3 knockdown cells to the level of si NS cells treated with SR141716 (Fig. 6b and d).

Knockdown of ATG7 blocks the effect of CB1 inhibition on autophagy

ATG7 is essential for the formation of autophagic vesicles and directly involved in the processing of LC3 (Mizushima

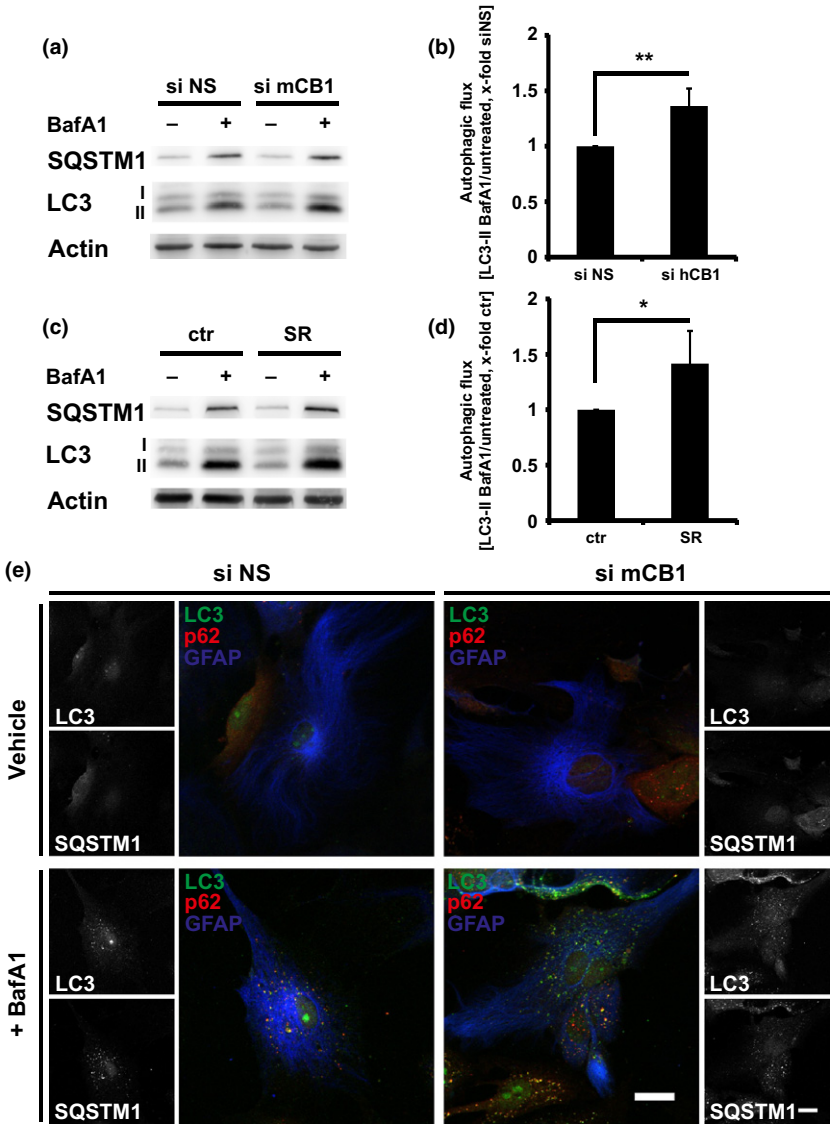

Fig. 4 Enhanced autophagic flux after cannabinoid Receptor 1 (CB1) knockdown in primary astrocytes. (a) Knockdown of CB1 expression led to an increased accumulation of light chain 3 protein (LC3)-II and sequestosome 1 (SQSTM1) in bafilomycin A1 (BafA1) treated (1 μM, 4 h) astrocytes. (b) The autophagic flux as measured by calculating the quotient of LC3-II level in BafA1 treated versus untreated cells was significantly enhanced in CB1 knockdown cells. Shown are the means ± SD ($n = 4$) (c) Astrocytes were treated with CB1 receptor antagonist SR141716 (SR, Rimonabant; 100 nM, 4 h) and lysosomal degradation was subsequently blocked by bafilomycin A1 (BafA1) treatment (1 μM, 4 h). (d) The autophagic flux was enhanced in SR treated cells. Shown are the means ± SD ($n = 5$). $^{*}p < 0.05$; $^{**}p < 0.01$. (e) Shown are maximum intensity projections of confocal laser scanning microscopy of nonsense siRNA [si nonsense (NS)] or CB1 siRNA (si mCB1) transfected astrocytes. Immunostaining visualizes LC3 (green), SQSTM1 (red), and GFAP (blue, to identify astrocytes individually). Scale bars = 20 μm.

et al. 2011) and as a consequence the knockdown of ATG7 (si ATG7, Fig. 7c) reduced the autophagic flux to 75% of si nonsense transfected cells (si NS, Fig. 7a and b). In contrast to the down-regulation of the regulatory BECLIN1-complex (Fig. 6), treatment with the CB1 antagonist Rimonabant (SR141716, 4 h 100 nM prior to BafA1 treatment) under ATG7 knockdown condition was not sufficient to induce the autophagic flux (Fig. 7a and b).

Despite its influence on the autophagic flux, CB1-knockdown does not alter lysosomal activity

It has been reported that intracellular CB1 influences lysosomal stability and activity under protein stress conditions and in CB1-KO mice (Noonan *et al.* 2010; Brailoiu *et al.* 2011; Piyanova *et al.* 2013). Therefore, we examined whether impaired lysosomal activity is responsible for the increased accumulation of LC3-II after BafA1 treatment in cells with reduced CB1 levels. Protein levels of the lysosomal marker lysosomal-associated membrane protein 1 did not change in nonsense siRNA (si NS) versus CB1 siRNA (si hCB1)-transfected cells measured by western blot analysis (Fig. 8a and b). Moreover, immunocytochemical stainings of an additional lysosomal marker lysosomal-associated membrane protein 2 were did not show differences in the lysosomal load of si hCB1-treated compared to si NS-treated cells (Fig. 8d). Nevertheless, lysosomes of si hCB1 cells showed a stronger colocalization with autophagic vesicles than lysosomes did in si NS control cells following BafA1 treatment (Fig. 8d). To investigate whether the lysosomal activity was altered after CB1 siRNA knockdown, we measured the enzymatic activity of lysosomal proteases using a cathepsin-specific substrate

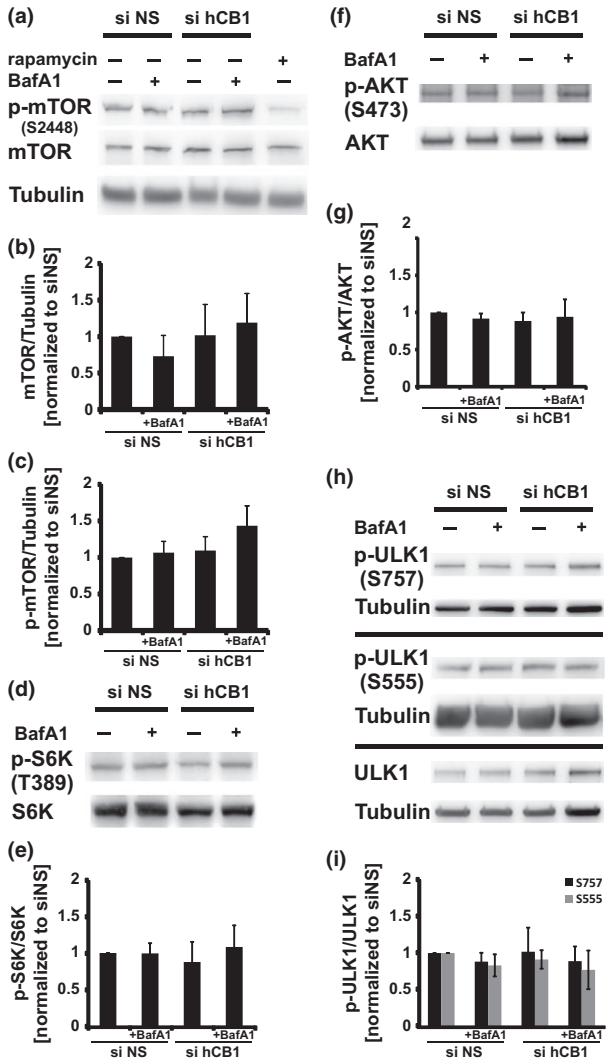

Fig. 5 Modulation of autophagic flux via cannabinoid Receptor 1 (CB1) is independent of mammalian target of rapamycin complex 1 (mTORC1). (a) CB1 siRNA-transfected cells (si hCB1) showed no alteration in mTOR-phosphorylation at S2448 (p-mTOR) compared to nonsense si RNA [si nonsense (NS)]-transfected cells. Rapamycin treatment (10 μM, 4 h) reduced p-mTOR level. (b) mTOR total protein (mTOR) or (c) p-mTOR were not significantly regulated between si CB1 and si NS cells. mTOR and p-mTOR was not altered by bafilomycin A1 (BafA1) treatment (1 μM, 4 h) compared to vehicle control. (d) western blot and (e) densitometric analysis of p70S6-kinase (S6K) and its phosphorylation at T389 (p-S6K), as well as serine/threonine protein kinase Akt (AKT)-phosphorylation at S473 (p-AKT) (f and g) and ULK1-phosphorylation at S757 and S555 (h and I) after CB1 knockdown revealed no difference. Shown are the means ± SD (n = 4).

(Z-RR-AMC). Interestingly, there was no difference in the lysosomal activity of cells with reduced CB1 expression versus control cells, but BafA1 treatment was sufficient to suppress the enzymatic activity of the lysosomal proteases to approximately 50% of vehicle controls in si NS and si hCB1 cells (Fig. 8c).

Discussion

In this study we describe a novel function of the cannabinoid receptor CB1 in the control of the autophagic flux. We suggest that CB1 activity modulates autophagic vesicle formation in a non-canonical, mTOR and BECLIN1-complex independent manner.

HEK cells and primary astrocytes expressing CB1 show a strong induction of autophagic vesicle formation upon reducing the level of the endogenous receptor via siRNA, whereas the expression of ATG genes is not altered. Interestingly, the proteasomal activity is not changed in those cells either, showing the specificity of CB1 signaling for the regulation of the autophagic flux. This is remarkable as the two cellular degradation systems are connected via molecular mediators (Gamerdinger *et al.* 2009) and seem to be regulated simultaneously under conditions of cellular stress (Korolchuk *et al.* 2009; Gamerdinger *et al.* 2011a). Pharmacological knockdown of CB1 activity using the CB1-specific antagonist Rimonabant mimics the effects of reducing CB1 mRNA whereas activation of CB1 using Win2 inhibits the autophagic flux. In this context, it is important to mention that HEK cells do not express CB2. Win2 is an agonist of both cannabinoid receptors and therefore its effect on the autophagic flux could be due to CB2 activity. However, stimulation of CB2 has been shown to induce autophagic activity by inducing endoplasmatic reticulum-stress in cancer cells in an mTOR-dependent fashion (Salazar *et al.* 2009a,b). Here, low doses (at least 50-fold lower) of cannabinoids and CB2-free cells (HEK) were utilized to avoid cannabinoid-dependent induction of autophagy in cancer cells (Vara *et al.* 2011), and also because cancer cells could react differently to cannabinoids than somatic and primary cells. In addition, the differential expression of CB1 and CB2 in various tissues (Galiegue *et al.* 1995; Howlett 2002; Walter *et al.* 2003; Osei-Hyiaman *et al.* 2005; Van Sickle *et al.* 2005; Onaivi *et al.* 2006) might contribute to cell type-specific fine tuning of autophagic activity mediated by endogenous cannabinoids, calling for further investigations.

The modulatory effects of CB1 manipulation on the autophagic activity of the cells were induced by genetic modification (siRNA transfection) as well as pharmacological treatment in a uniform manner. This suggests that the alteration of the autophagic flux is based on CB1 activity and not on a direct interaction of CB1 protein with an autophagy-inducing agent. Moreover, transient over-expression of CB1 protein had no effect on the autophagic flux (data not shown), suggesting CB1 activity and not a protein-protein interaction involving CB1 as the causative mode of action.

Two multiprotein complexes are involved in the canonical induction pathway of autophagic vesicle formation: mTOR- and BECLIN1-complex. While mTORC1 negatively regulates autophagy and its inhibition consequently drives autophagic

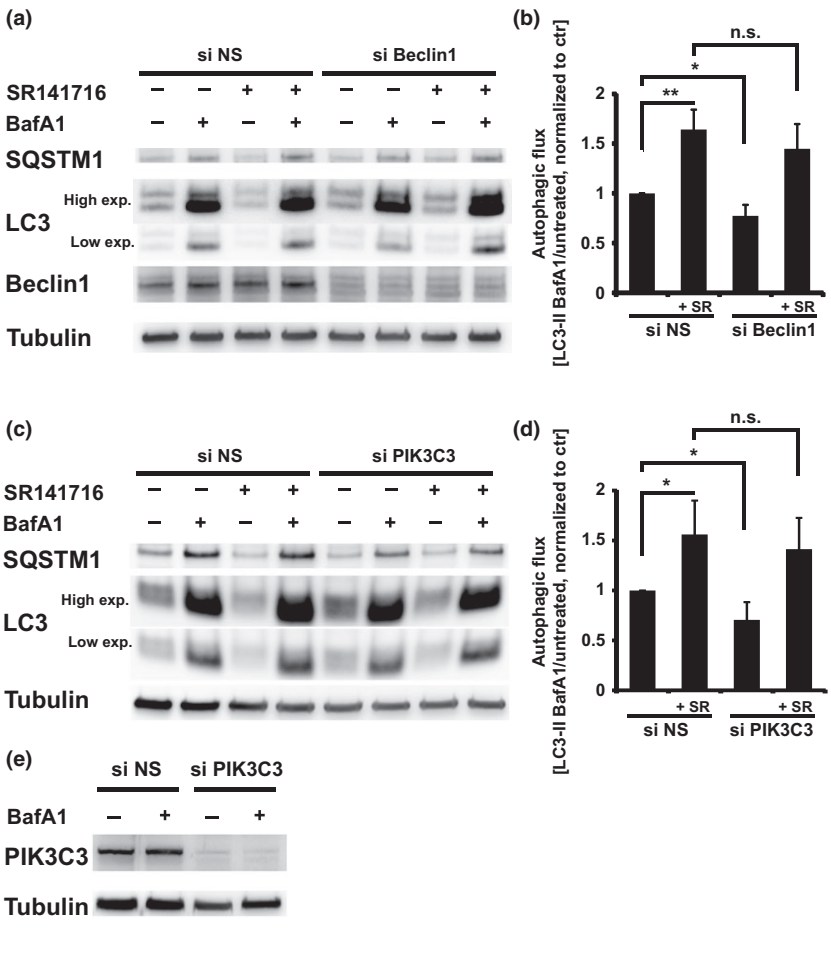

Fig. 6 Knockdown of coiled-coil myosin-like BCL2-interacting protein 1 (BECLIN1)/class III PI3-kinase (PIK3C3) – complex inhibits autophagic vesicle formation which can be restored by Rimonabant treatment. Bafilomycin A1 (BafA1) treatment (1 μM, 4 h) of cells transfected with (a) BECLIN1 (si BECLIN1) or (c) PIK3C3 (siPIK3C3) siRNA led to a reduced accumulation of light chain 3 protein (LC3)-II compared to nonsense si RNA [si nonsense (NS)] transfected cells. (b) The autophagic flux was equally enhanced in si NS and (b) si BECLIN1 or (d) siPIK3C3 cells by Rimonabant (SR141716, 4 h 100 nM) treatment compared to vehicle controls. (e) western blot analysis of PIK3C3 knockdown efficiency. Shown are the means ± SD ($n = 4$), n.s. = no significance; *$p < 0.05$; **$p < 0.01$.

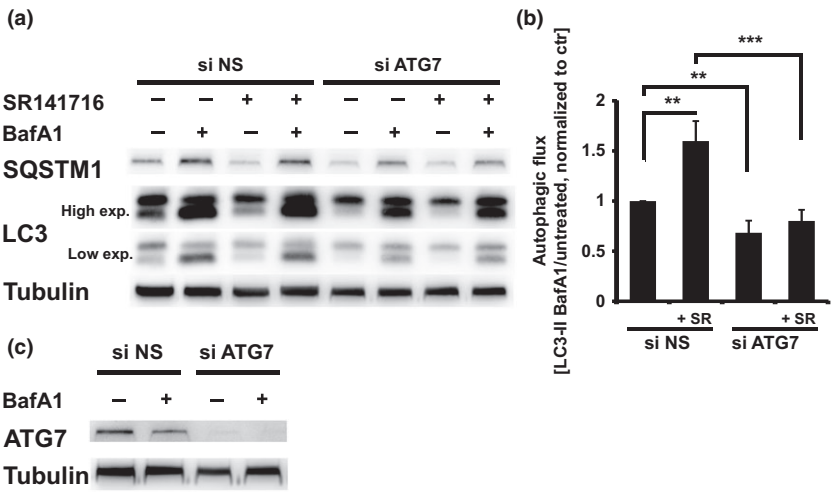

Fig. 7 Rimonabant treatment does not alter inhibited autophagic vesicle formation in si autophagy-related (ATG)7-transfected cells. (a) Bafilomycin A1 (BafA1) treatment (1 μM, 4 h) of cells transfected with ATG7 (si ATG7) led to a reduced accumulation of light chain 3 protein (LC3)-II compared to nonsense si RNA [si nonsense (NS)] transfected cells. (b) The autophagic flux remains reduced in si ATG7 cells after Rimonabant (SR141716, 4 h 100 nM) treatment. (c) Western blot analysis of ATG7 knockdown efficiency. Shown are the means ± SD ($n = 4$), **$p < 0.01$; ***$p < 0.001$.

flux (Klionsky *et al.* 2012), the BECLIN1-complex induces autophagic activity in most physiological states (Fimia *et al.* 2007; Itakura *et al.* 2008; Zhong *et al.* 2009). mTOR integrates different cellular signals that are known to be modulated by CB1 activity (e.g. AKT-kinase or mitogen activated kinase/extracellular regulated MAP kinase signaling), which alter the phosphorylation state of the mTOR-kinase itself and thus influence autophagic activity. Dando *et al.* (2013) recently showed that high dosages of CB1 agonist arachidonoyl cyclopropamide induce autophagy in pancreatic cancer cells in an AMPK-mTOR-dependent manner. However, our data show no altered mTOR-phosphorylation after CB1 modulation, which excludes upstream signaling cascades as causative for the altered autophagic flux. One

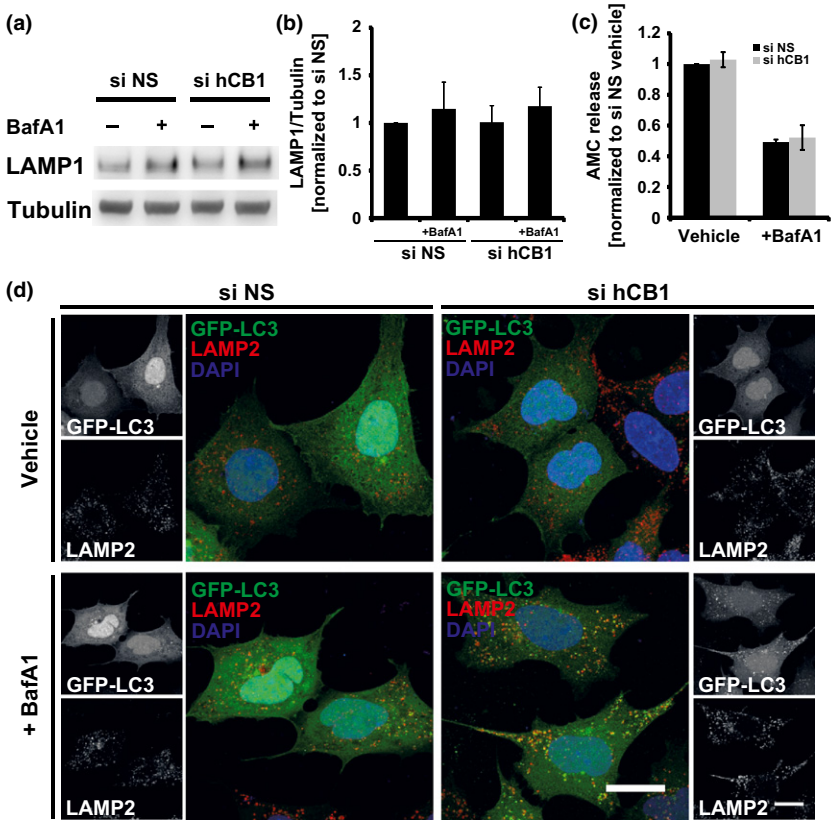

Fig. 8 Lysosomal activity remains unchanged after cannabinoid Receptor 1 (CB1) knockdown. (a) Western blot analysis of the lysosomal marker lysosomal-associated membrane protein 1 (LAMP1) revealed no difference between CB1 siRNA (si hCB1) and nonsense siRNA [si nonsense (NS)] transfected cells. (b) LAMP1 protein level was not significantly altered in si hCB1 compared to si NS cells after bafilomycin A1 (BafA1) treatment (1 μM, 4 h). (c) Lysosomal activity was measured using a substrate specific for lysosomal cathepsin (Z-RR-AMC). BafA1 treatment equally reduced lysosomal activity in si hCB1 and si NS cells by approximately 50%. Shown are the means ± SD ($n = 3$), with no statistical significant difference. (d) Maximum intensity projections of confocal laser scanning microscopy revealed enhanced colocalization of lysosomal-associated membrane protein 2 (LAMP2)- and light chain 3 protein (LC3)-positive structures in si hCB1 compared to si NS cells. Cells were cotransfected with green-flourescent protein (GFP)-LC3 expression plasmid to indicate successfully transfected cells and LC3 distribution within the cells (green). Lysosomes were immunostained with the marker LAMP2 (red). Scale bars = 20 μm.

important upstream modulator of mTOR activity is AKT and this kinase is involved in cannabinoid-induced and CB2-dependent autophagy (Salazar *et al.* 2009a,b). In turn, CB1 can modulate AKT activity (Cannich *et al.* 2004; Ozaita *et al.* 2007). However, in our transient CB1 knockdown paradigm we could not observe CB1-dependent modulation of AKT. Moreover, the phosphorylation of the relevant downstream target of mTOR, the ULK1 kinase, which is directly involved in the initiation of autophagic vesicle formation (Mizushima 2010), remained unaltered after CB1 knockdown. Since AMPK is able to phosphorylate ULK1 (Egan *et al.* 2011) bypassing mTORC1 signaling, we investigated whether this pathway might be relevant in the present context. Again ULK1-phosphorylation remained unaltered. Moreover, another substrate of mTOR, the p70S6 kinase (S6K) (Dufner and Thomas 1999), showed no difference in its phosphorylation status after CB1 knockdown. Thus, our data suggest that CB1 influences the autophagic flux independently of the mTORC1-signaling. A recent study in CB1-KO mice reported no differences in AKT and mTOR signaling, which supports our conclusion (Piyanova *et al.* 2013). Knocking down BECLIN1 as the central protein to form a functional BECLIN1-complex, or PIK3C3 as the relevant kinase of this complex, expectedly reduced the autophagic flux. Inhibiting CB1 activity with Rimonabant restored the autophagic flux to the level of the control condition, which speaks against the involvement of the BECLIN1-complex in CB1-mediated modulation of autophagic vesicle formation. Evidence emerges that the canonical induction pathways of autophagy are not the exclusive ones. Recent reports show alternative induction pathways which do not include the whole canonical machinery (reviewed in Codogno *et al.* 2012). On the basis of

our data, we propose that CB1 likewise modulates autophagic flux non-canonically, although the detailed intracellular signaling cascade is yet unclear. Disturbing autophagic vesicle formation by knocking down ATG7 as an essential component of autophagosome biogenesis prevented the CB1-dependent modulation of the autophagic flux completely. The key components of the autophagic machinery are yet to be identified. It is far beyond the aims of this study to reveal the complete signaling pathway involved. This should be subjected to further investigations as CB1 activity specifically affects the regulation of the autophagic vesicle formation without modulating downstream cellular processes like lysosomal activity, and could be used as a novel pharmacological target.

Autophagic pathways cannot be considered completely autonomous from lysosomal activity, since autophagic vesicles are cleared via lysosomal degradation. On the other hand, the induction of the autophagic flux is not directly linked to enhanced lysosomal activity (Li *et al.* 2013). However, standard methods for measuring autophagic activity rely on the blockade of lysosomal degradation and thus inhibition of the clearance of autophagic vesicles (Klionsky *et al.* 2012). In prior studies targeting the issue of a potential influence of the CB1 on autophagic activity and revealing a CB1-dependent induction of autophagy, these important inhibition experiments are missing (recently Dando *et al.* 2013). In contrast to these studies, Piyanova *et al.* (2013) showed that the autophagic flux is enhanced in neuronal cultures of mice lacking CB1. In line with this finding, we could demonstrate in this study that this effect is not specific to these transgenic animals. The transient knockdown of CB1 as well as treatment with Rimonabant at low concentration is sufficient to induce the autophagic flux in HEK cells and primary astrocytes. Although CB1 knockdown in HEK cells was not as efficient as in primary astrocytes, HEK cells reacted more sensitively to the modulation of CB1 activity. Despite some variance, the CB1-dependent modulation of the autophagic flux might be a general physiological function in different cell types. As discussed above, the observed enhanced accumulation of LC3-II after CB1 inhibition or BafA1 treatment could be due to an enhanced autophagic flux as well as disturbed lysosomal activity. Since active intracellular CB1 is present in the lysosomal membrane (Brailoiu *et al.* 2011), CB1 might support lysosomal degradation processes directly. Thus, its lysosomal location seems to be linked to a physiological function beyond the degradation via the autophagosomal/lysosomal system (He *et al.* 2013). We did neither observe a reduced amount nor activity (measured through cathepsins, the activity substrate of lysosomal proteases) of lysosomes in cells with lower CB1 expression. These findings argue against previous observations suggesting that CB1 activation supports lysosomal function under amyloid-β-mediated protein stress or in mice lacking CB1 (Noonan *et al.* 2010; Piyanova *et al.* 2013). In our cellular model we did not use exogenic protein stress to study the influence of CB1 activity on autophagic vesicle formation, but represented physiological baseline conditions. The cellular toxicity exerted by the amyloid-β peptide alters the lysosomal/autophagosomal system (reviewed in Morawe *et al.* 2012), thus the opposing results might be explained by an additional effect of CB1 activation and amyloid-β toxicity in this protein stress paradigm. The reduction in lysosomal activity in CB1-KO mice (independent of the amount of lysosomes) could be due to developmental adaptations in those transgenic animals. Alternatively, it could be due to neuron-specific effects as lysosomal activity was measured in neuronal tissue (Piyanova *et al.* 2013). In contrast, in our study CB1 activity was reduced by transient siRNA knockdown, leaving lysosomal activity unaltered, suggesting a specific effect of CB1 activity on the regulation of the autophagic vesicle formation without effecting downstream cellular processes like lysosomal degradation. In addition, some cell types (like neurons) might be particularly sensitive to CB1-dependent modulation of the lysosomal system (Nixon 2013).

Autophagy is involved in many important aspects of cellular physiology of which the reaction on different nutrient states of the cell is one of the most prominent and conserved. CB1 plays an important role in appetite control as well as in metabolic processes independent of food intake (Cota *et al.* 2003; Ravinet Trillou *et al.* 2004; Cavuoto *et al.* 2007). In this study we provide first evidence that modulation of the autophagic flux via CB1 might be relevant for cells to stabilize homeostasis under nutrient (amino acid) starvation and proteostatic stress. Moreover, our data suggest an involvement of CB1 activity specifically in the control of the autophagic flux without altering the expression of autophagy-relevant genes nor the activity of the UPS. These findings are consistent with the emerging evidence for a direct influence of CB1 activity on the energy metabolism (Benard *et al.* 2012; O'Keefe *et al.* 2013).

Acknowledgments and conflict of interest disclosure

The authors would like to thank B.Lutz for providing SR141716 (Rimonabant); T. Morawe, A. Kern, and C. Ziegler for helpful comments on the manuscript. This work was performed in the framework of the DFG research group (DFG FOR 926, grant to C.B.) and was further supported by the Peter and Beate Heller Foundation and the Corona Foundation (grants to C.B.). The authors declare that they have no conflict of interest. *Ethical standards*: The authors declare that the experiments comply with the current laws of Germany.

All experiments were conducted in compliance with the ARRIVE guidelines.

Supporting information

Additional supporting information may be found in the online version of this article at the publisher's web-site:

Figure S1. LC3 conversion after CB1 knockdown, PepA/E64d treatment and HEK::D2eGFP cells.

Figure S2. Starvation experiments in HEK cells.

Figure S3. Residual level of CB1 mRNA after CB1 siRNA treatment and LC3-punctae count.

Table S1. Antibodies used for this study.

Table S2. Small interfering RNA (siRNA) and PCR-primer sequences used in this study.

Table S3. CB1 knockdown does not alter the expression of autophagy-related genes.

References

Benard G., Massa F., Puente N. *et al.* (2012) Mitochondrial CB(1) receptors regulate neuronal energy metabolism. *Nat. Neurosci.* **15**, 558–564.

Brailoiu G. C., Oprea T. I., Zhao P., Abood M. E. and Brailoiu E. (2011) Intracellular cannabinoid type 1 (CB1) receptors are activated by anandamide. *J. Biol. Chem.* **286**, 29166–29174.

Cannich A., Wotjak C. T., Kamprath K., Hermann H., Lutz B. and Marsicano G. (2004) CB1 cannabinoid receptors modulate kinase and phosphatase activity during extinction of conditioned fear in mice. *Learn. Mem.* **11**, 625–632.

Cavuoto P., McAinch A. J., Hatzinikolas G., Cameron-Smith D. and Wittert G. A. (2007) Effects of cannabinoid receptors on skeletal muscle oxidative pathways. *Mol. Cell. Endocrinol.* **267**, 63–69.

Chiang G. G. and Abraham R. T. (2005) Phosphorylation of mammalian target of rapamycin (mTOR) at Ser-2448 is mediated by p70S6 kinase. *J. Biol. Chem.* **280**, 25485–25490.

Clague M. J. and Urbe S. (2010) Ubiquitin: same molecule, different degradation pathways. *Cell* **143**, 682–685.

Codogno P., Mehrpour M. and Proikas-Cezanne T. (2012) Canonical and non-canonical autophagy: variations on a common theme of self-eating? *Nat. Rev. Mol. Cell Biol.* **13**, 7–12.

Cota D., Marsicano G., Tschop M. *et al.* (2003) The endogenous cannabinoid system affects energy balance via central orexigenic drive and peripheral lipogenesis. *J. Clin. Investig.* **112**, 423–431.

Dando I., Donadelli M., Costanzo C., Dalla Pozza E., D'Alessandro A., Zolla L. and Palmieri M. (2013) Cannabinoids inhibit energetic metabolism and induce AMPK-dependent autophagy in pancreatic cancer cells. *Cell Death Dis.* **4**, e664.

Devane W. A., Dysarz F. A., 3rd, Johnson M. R., Melvin L. S. and Howlett A. C. (1988) Determination and characterization of a cannabinoid receptor in rat brain. *Mol. Pharmacol.* **34**, 605–613.

Dibble C. C. and Manning B. D. (2013) Signal integration by mTORC1 coordinates nutrient input with biosynthetic output. *Nat. Cell Biol.* **15**, 555–564.

Dufner A. and Thomas G. (1999) Ribosomal S6 kinase signaling and the control of translation. *Exp. Cell Res.* **253**, 100–109.

Egan D. F., Shackelford D. B., Mihaylova M. M. *et al.* (2011) Phosphorylation of ULK1 (hATG1) by AMP-activated protein kinase connects energy sensing to mitophagy. *Science* **331**, 456–461.

Fimia G. M., Stoykova A., Romagnoli A. *et al.* (2007) Ambra1 regulates autophagy and development of the nervous system. *Nature* **447**, 1121–1125.

Galiegue S., Mary S., Marchand J. *et al.* (1995) Expression of central and peripheral cannabinoid receptors in human immune tissues and leukocyte subpopulations. *Eur. J. Biochem.* **232**, 54–61.

Gamerdinger M., Hajieva P., Kaya A. M., Wolfrum U., Hartl F. U. and Behl C. (2009) Protein quality control during aging involves recruitment of the macroautophagy pathway by BAG3. *EMBO J.* **28**, 889–901.

Gamerdinger M., Carra S. and Behl C. (2011a) Emerging roles of molecular chaperones and co-chaperones in selective autophagy: focus on BAG proteins. *J. Mol. Med.* **89**, 1175–1182.

Gamerdinger M., Kaya A. M., Wolfrum U., Clement A. M. and Behl C. (2011b) BAG3 mediates chaperone-based aggresome-targeting and selective autophagy of misfolded proteins. *EMBO Rep.* **12**, 149–156.

Graham F. L. and van der Eb A. J. (1973) Transformation of rat cells by DNA of human adenovirus 5. *Virology* **54**, 536–539.

He C., Wei Y., Sun K. *et al.* (2013) Beclin 2 functions in autophagy, degradation of g protein-coupled receptors, and metabolism. *Cell* **154**, 1085–1099.

Howlett A. C. (2002) The cannabinoid receptors. *Prostaglandins Other Lipid Mediat.* **68–69**, 619–631.

Itakura E., Kishi C., Inoue K. and Mizushima N. (2008) Beclin 1 forms two distinct phosphatidylinositol 3-kinase complexes with mammalian Atg14 and UVRAG. *Mol. Biol. Cell* **19**, 5360–5372.

Jackson W. T., Giddings T. H., Jr, Taylor M. P., Mulinyawe S., Rabinovitch M., Kopito R. R. and Kirkegaard K. (2005) Subversion of cellular autophagosomal machinery by RNA viruses. *PLoS Biol.* **3**, e156.

Kirkin V., McEwan D. G., Novak I. and Dikic I. (2009) A role for ubiquitin in selective autophagy. *Mol. Cell* **34**, 259–269.

Klionsky D. J., Abdalla F. C., Abeliovich H. *et al.* (2012) Guidelines for the use and interpretation of assays for monitoring autophagy. *Autophagy* **8**, 445–544.

Korolchuk V. I., Mansilla A., Menzies F. M. and Rubinsztein D. C. (2009) Autophagy inhibition compromises degradation of ubiquitin-proteasome pathway substrates. *Mol. Cell* **33**, 517–527.

Li M., Khambu B., Zhang H. *et al.* (2013) Suppression of lysosome function induces autophagy via a feedback down-regulation of MTORC1 activity. *J. Biol. Chem.*, **288**, 35769–35780.

Matsuda L. A., Lolait S. J., Brownstein M. J., Young A. C. and Bonner T. I. (1990) Structure of a cannabinoid receptor and functional expression of the cloned cDNA. *Nature* **346**, 561–564.

Mechoulam R. and Gaoni Y. (1965) A total synthesis of Dl-delta-1-tetrahydrocannabinol, the active constituent of hashish. *J. Am. Chem. Soc.* **87**, 3273–3275.

Mizushima N. (2010) The role of the Atg1/ULK1 complex in autophagy regulation. *Curr. Opin. Cell Biol.* **22**, 132–139.

Mizushima N., Yoshimori T. and Ohsumi Y. (2011) The role of Atg proteins in autophagosome formation. *Annu. Rev. Cell Dev. Biol.* **27**, 107–132.

Morawe T., Hiebel C., Kern A. and Behl C. (2012) Protein homeostasis, aging and Alzheimer's disease. *Mol. Neurobiol.* **46**, 41–54.

Munro S., Thomas K. L. and Abu-Shaar M. (1993) Molecular characterization of a peripheral receptor for cannabinoids. *Nature* **365**, 61–65.

Nixon R. A. (2013) The role of autophagy in neurodegenerative disease. *Nat. Med.* **19**, 983–997.

Noonan J., Tanveer R., Klompas A., Gowran A., McKiernan J. and Campbell V. A. (2010) Endocannabinoids prevent beta-amyloid-mediated lysosomal destabilization in cultured neurons. *J. Biol. Chem.* **285**, 38543–38554.

O'Keefe L., Simcocks A. C., Hryciw D. H., Mathai M. L. and McAinch A. J. (2013) The cannabinoid receptor 1 and its role in influencing peripheral metabolism. *Diabetes Obes. Metab.* **16**, 294–304.

Onaivi E. S., Ishiguro H., Gong J. P. *et al.* (2006) Discovery of the presence and functional expression of cannabinoid CB2 receptors in brain. *Ann. N. Y. Acad. Sci.* **1074**, 514–536.

Osei-Hyiaman D., DePetrillo M., Pacher P. *et al.* (2005) Endocannabinoid activation at hepatic CB1 receptors stimulates fatty acid synthesis and contributes to diet-induced obesity. *J. Clin. Investig.* **115**, 1298–1305.

Ozaita A., Puighermanal E. and Maldonado R. (2007) Regulation of PI3K/Akt/GSK-3 pathway by cannabinoids in the brain. *J. Neurochem.* **102**, 1105–1114.

Pankiv S., Clausen T. H., Lamark T., Brech A., Bruun J. A., Outzen H., Overvatn A., Bjorkoy G. and Johansen T. (2007) p62/SQSTM1 binds directly to Atg8/LC3 to facilitate degradation of ubiquitinated protein aggregates by autophagy. *J. Biol. Chem.* **282**, 24131–24145.

Pfaffl M. W., Horgan G. W. and Dempfle L. (2002) Relative expression software tool (REST) for group-wise comparison and statistical analysis of relative expression results in real-time PCR. *Nucleic Acids Res.* **30**, e36.

Piyanova A., Albayram O., Rossi C. A., Farwanah H., Michel K., Nicotera P., Sandhoff K. and Bilkei-Gorzo A. (2013) Loss of CB1 receptors leads to decreased cathepsin D levels and accelerated lipofuscin accumulation in the hippocampus. *Mech. Ageing Dev.* **134**, 391–399.

Ravinet Trillou C., Delgorge C., Menet C., Arnone M. and Soubrie P. (2004) CB1 cannabinoid receptor knockout in mice leads to leanness, resistance to diet-induced obesity and enhanced leptin sensitivity. *Int. J. Obes. Relat. Metab. Disord.* **28**, 640–648.

Salazar M., Carracedo A., Salanueva I. J. *et al.* (2009a) TRB3 links ER stress to autophagy in cannabinoid anti-tumoral action. *Autophagy* **5**, 1048–1049.

Salazar M., Carracedo A., Salanueva I. J. *et al.* (2009b) Cannabinoid action induces autophagy-mediated cell death through stimulation of ER stress in human glioma cells. *J. Clin. Investig.* **119**, 1359–1372.

Stumm C., Hiebel C., Hanstein R., Purrio M., Nagel H., Conrad A., Lutz B., Behl C. and Clement A. B. (2013) Cannabinoid receptor 1 deficiency in a mouse model of Alzheimer's disease leads to enhanced cognitive impairment despite of a reduction in amyloid deposition. *Neurobiol. Aging* **34**, 2574–2584.

Tanida I. (2011) Autophagosome formation and molecular mechanism of autophagy. *Antioxid. Redox Signal.* **14**, 2201–2214.

Van Sickle M. D., Duncan M., Kingsley P. J. *et al.* (2005) Identification and functional characterization of brainstem cannabinoid CB2 receptors. *Science* **310**, 329–332.

Vara D., Salazar M., Olea-Herrero N., Guzman M., Velasco G. and Diaz-Laviada I. (2011) Anti-tumoral action of cannabinoids on hepatocellular carcinoma: role of AMPK-dependent activation of autophagy. *Cell Death Differ.* **18**, 1099–1111.

Walter L., Franklin A., Witting A., Wade C., Xie Y., Kunos G., Mackie K. and Stella N. (2003) Nonpsychotropic cannabinoid receptors regulate microglial cell migration. *J. Neurosci.* **23**, 1398–1405.

Wilson R. I. and Nicoll R. A. (2001) Endogenous cannabinoids mediate retrograde signalling at hippocampal synapses. *Nature* **410**, 588–592.

Witan H., Kern A., Koziollek-Drechsler I., Wade R., Behl C. and Clement A. M. (2008) Heterodimer formation of wild-type and amyotrophic lateral sclerosis-causing mutant Cu/Zn-superoxide dismutase induces toxicity independent of protein aggregation. *Hum. Mol. Genet.* **17**, 1373–1385.

Zhong Y., Wang Q. J., Li X., Yan Y., Backer J. M., Chait B. T., Heintz N. and Yue Z. (2009) Distinct regulation of autophagic activity by Atg14L and Rubicon associated with Beclin 1-phosphatidylinositol-3-kinase complex. *Nat. Cell Biol.* **11**, 468–476.

Zschocke J., Bayatti N. and Behl C. (2005) Caveolin and GLT-1 gene expression is reciprocally regulated in primary astrocytes: association of GLT-1 with non-caveolar lipid rafts. *Glia* **49**, 275–287.